Evaluation of an Automatic Free Fall SPT Hammer system

by

J.P. Kaushish*

D.K. Gautam*

A.K. Jethi**

Mahendra Pal**

Introduction

Studies on Standard Penetration Test (SPT) for its use in soil exploration and its performance in respect of predicting different soil characteristics have been a matter of great concern for the geotechnical engineers. This is obvious from the fact that during the last two decades the ASTM Standard Penetration Test and Split-Barrel Sampling of Soils (D 1586) have been reevaluated by several investigators (Flecher 1965, Dinesh Mohan et al. 1970, Sanglerat, 1972, Schmertmann 1978, Kovacs et al. 1981, 1983). Some of the conclusions and ensuing discussions have however, indicated a definite need for the control of field procedures and use of better equipments during the performance of SPT because a wide variation in N values has been reported by the investigators in the field tests. The primary cause of such a large variation in N values is attributed to large variations in the man-machine systems and procedures adopted at different work sites.

In India the SPT is conducted manually by dropping a free falling hammer (63.5 kg) from a height of 76.2 cm on an anvil fitted atop the drill rod assembly which also carries a sampler at its bottom end (1). Because of the manual hoisting of the hammer, it is not always possible in practice to lift the hammer exactly to a height of 76.2 cm. This causes variations in the potential energy of the hammer and consequently in the impact kinetic energy of hammer on the anvil. The method of ensuring free fall of hammer is another source of variability. A large variation in the delivered impact energy results in practice because the SPT is invariably conducted using a manila rope and a rotating cathead system wherein to raise the hammer, the operator 'pulls' the free end of the rope towards himself until the prescribed fall height is seemingly achieved; to drop the hammer, the operator releases the rope around the revolving cathead by 'pushing' the rope into the cathead (Fig. 1). It is therefore obvious that in this system, the velocity of falling hammer before impact on the anvil will mostly depend on 'how' the operator releases (or pushes) the rope into the cathead. Yet another significant factor that adversely affects the impact energy of hammer is the complete absence of any device for maintaining alignment and verticality of the drill rod

* Scientist
** Scientific Assistant
} Central Building Research Institute, Roorkee, India.

(The revised manuscript of this paper was received in December, 1985 and is open for discussion till the end of June, 1986)

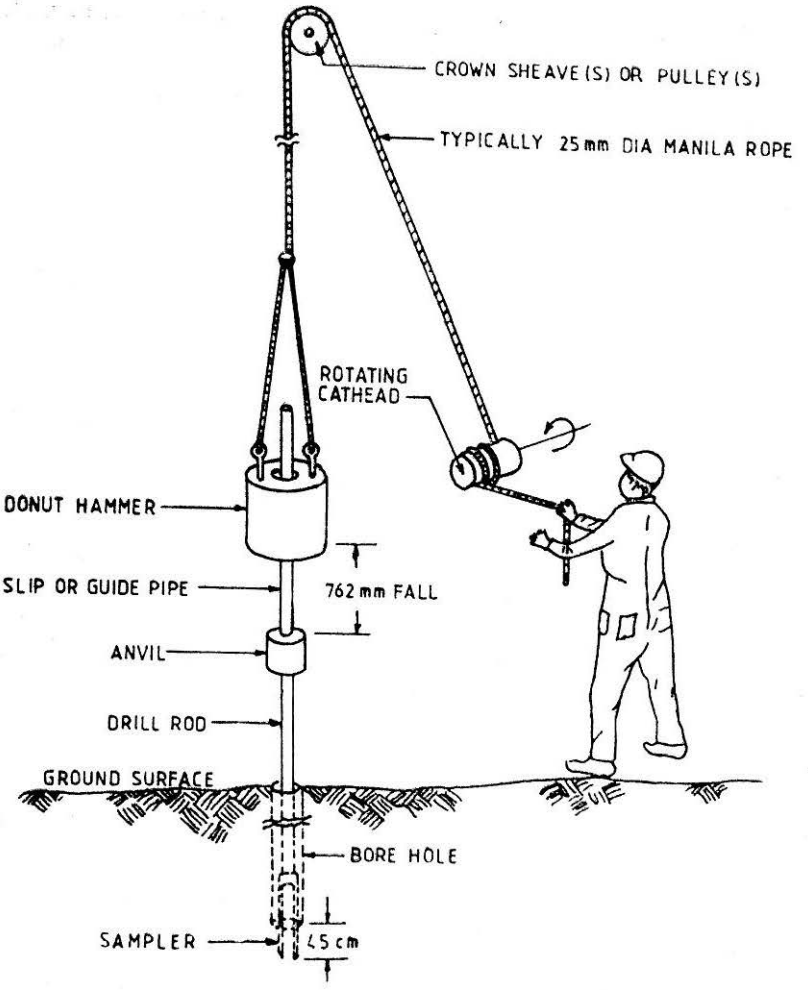

FIGURE 1 Illustrating the Prevalent Manual Method of Conducting SPT with Donut Hammer and Cathead and Rope system.

assembly with respect to the sampler during the dropping of hammer. Because of non-verticality of the drill rod assembly an additional frictional resistance occurs in the path of dropping hammer.

A necessary prerequisite for the continued use of the SPT is therefore an improvement of its reliability. To overcome the drawbacks of the manual SPT system presently used in India and elsewhere, the CBRI took up the development of an automatic free fall SPT hammer. The prototype has been successfully tried. It ensures conducting SPT according to the stipulations of the relevant IS Code.

Salient Features of the Automatic Free Fall SPT Hammer Developed at CBRI

The three principal objectives kept in view while designing the hammer are :

(*i*) It should provide reproducible SPT impact energy in each blow irrespective of the fact whether the hammer is operated manually or by power.

(*ii*) It should provide optimum safety in the man-machine system.

(*iii*) The system should be compact and economical to procure and operate.

The CBRI automatic free fall SPT hammer system comprises of a 63.5 kg Donut type hammer (18) (Fig. 2), an anvil (4) screwed with the top end of a drill rod assembly (3) which carries a split spoon sampler at its bottom end. A hammer guide rod (6) with its one end screwed with the anvil (4), is kept aligned with drill rod assembly (3) by a top plate (12). The top plate (12) is bolted with two vertical pipes (17) which at their lower end are coupled with the arms of anvil (4). The hammer (18) has a rigidly connected counter-headed cap (8) to facilitate holding and lifting of the hammer (18) with the help of a lifting lever assembly (9) through a set of roller-levers (16) which are hinged at position (7) with a support bolted with the base plate of the lifting lever assembly (9). Hoisting of the hammer (18) through the lifting lever assembly (9) is effected with the help of two hoisting rods (13) which are pulled up during hoisting with a rope that passes over a pulley (15) hanged from the vertex of a tripod (14). The hoisting rope finally goes to a winch which may be operated manually or by power. A set of tapered wedges (11) has been arranged at a suitable height to limit the hoisting of the hammer beyond a preset height of 76.2 cm in each stroke. During hoisting, the outwardly projecting end of lifting lever (16) comes in contact with the wedges (11) thereby making the lifting lever (16) to revolve about hinge point (7) and thus finally rendering the lifting lever (16) out of contact with counter headed cap (8) of the hammer (18). This results in setting the hammer (18) free to fall under gravity.

To ensure that outwardly end of the lifting lever (16) is always in line of contact (in the vertical plane) with the tapered wedge (11) for releasing the hammer (18), the rotation of the lifting lever assembly (9) (carrying the lifting levers (16)) about the hammer guide rod (6) is checked with a key (10) held rigidly with the lifting lever assembly (9). A key-way is milled in the hammer guide rod (6) to help movement of the key (10) only in the vertical direction. The springs provided help in easy engagement of the lifting lever (16) with the counter headed cap (8).

The vertical pipes (17) carry two rollers (5) which are capable of sliding along a track (19) fixed with a vertical guide frame (20). The assembly of track (19) and guide frame (20) has a base plate which is bolted with a wooden clamp (21) which is fixed during operation at the top end of the casing pipe (2) lowered in bore hole (1). The verticality and concentricity of hammer (18) with respect to drill rod assembly (3) is ensured through a well lubricated pair of bushes housed inside the counter head cap (8). During up and down movement of the hammer (18), the bushes while sliding along the hammer guide rod (6) keep the hammer (18) concentric with the hammer guide rod (18) which in turn is kept vertical and concentric with drill rod assembly (3) through a system comprising of top plate (12), vertical pipes (17), rollers (5), track (19) and the guide frame (20) mounted on the wooden clamp (21).

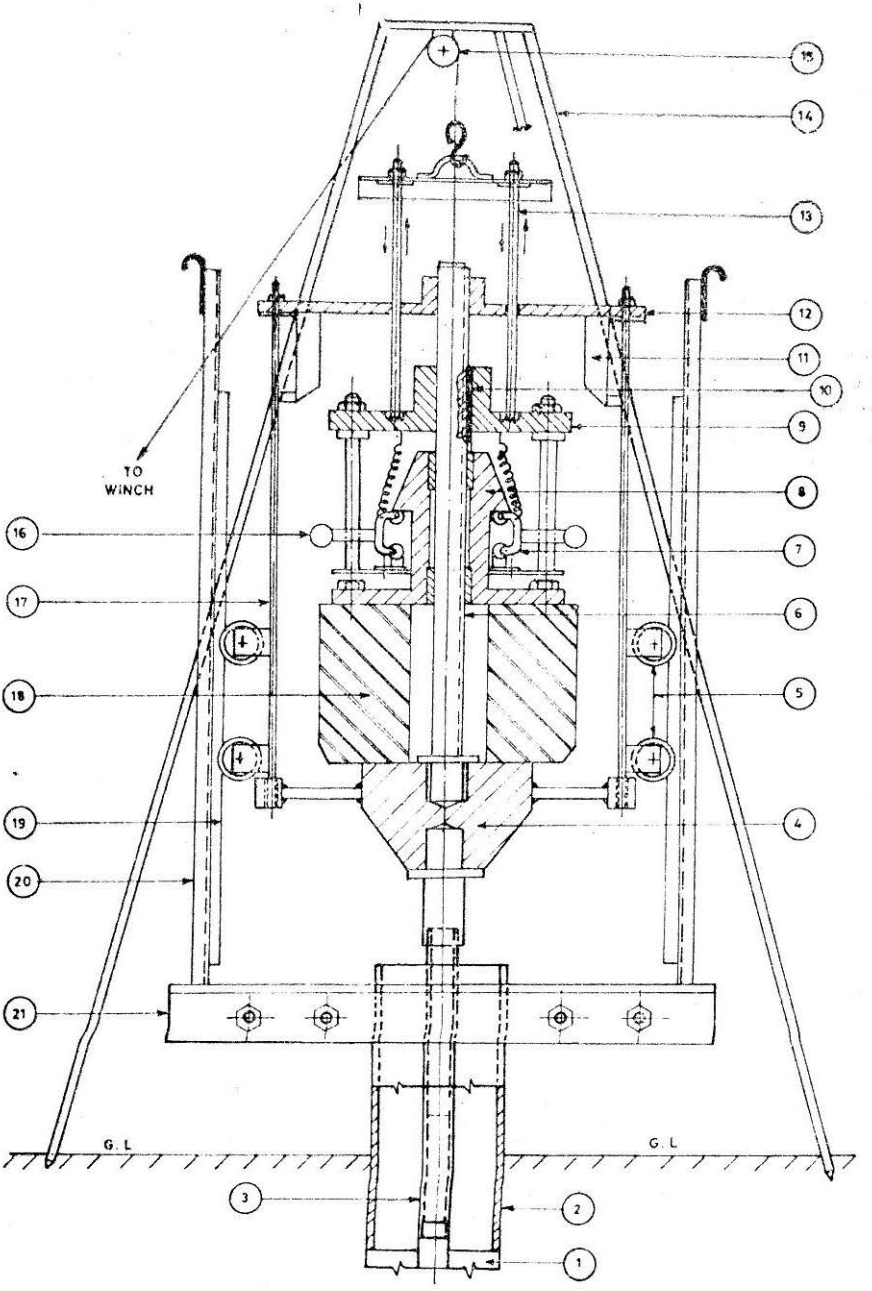

FIGURE 2 Showing the Details of Free Fall SPT Hammer Developed at CBRI.

Performance Evaluation Tests

Number of tests designed for evaluating the performance of CBRI automatic free fall SPT hammer were aimed at the quantification of the extent to which the developed system provides free gravity fall of the hammer.

The tests mainly included determination of actual fall height of the hammer, time of fall and the impact velocity of hammer. The data thus collected finally helped in determining and comparing the energy-ratio for velocity (or the efficiency) of the developed system with a theoretical system of true gravity fall.

Instrumentation

The test instrumentation set-up comprised of a galvanometric amplifier recorder (10) (Fig. 3), two light beam sensors or scanners (3 & 4) installed on a mounting frame (1) above the anvil (8) at a distance of 76.2 cm for sensing the target movement and two light beam projectors mounted on a frame (2). The hammer is covered with a zebra target (7) having alternate white and black strips. The galvanometric amplifier recorder (10) was a two channel unit with a built-in solid state amplifier and a curvilinear type pen recorder for each channel. The scanner (3 or 4) was a photo-conductive cell having resistance variations of 5 to 5.6 k

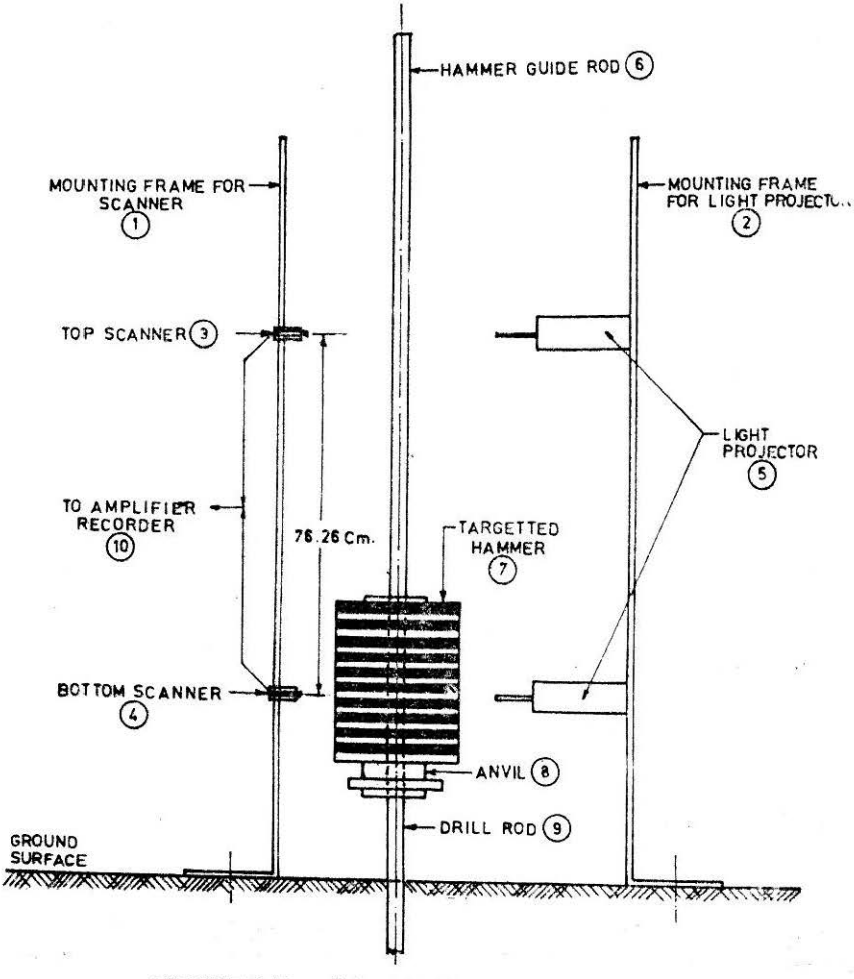

FIGURE 3 Essentials of the Test Instrumentation Set-up.

ohms. The light beam projector (5) comprised of a 200 watt coiled—filament type clear bulb mounted in a 60 cm long three piece telescopic barrel of 12 cm bore and made of tin sheet painted Matt black internally and having a 6 mm wide horizontal slit at the other end of barrel for directing a controlled width beam on to the target. The target wrapped around the hammer was made of 25×45 cm drawing sheet which was painted with alternate 1.25 cm wide white and black horizontal strips.

The instrumentation essentially utilized the Wheat stone bridge principle in conjunction with photo-conductive cell. As shown in Fig. 4, the bridge arms CB and BD consist of two fixed resistances (Q&S) of equal value; arm AD has a variable resistance R (for balancing the bridge) and arm AC has a fixed resistance P in series with a photo-conductive cell Pc. With a fixed potential applied across AC and Pc receiving a fixed amount of light, the balance resistor R is so adjusted that it becomes equal to resistance $P + P_c$. The bridge is then balanced, hence no current flows through G. During trials, the light beam from light projector (5) (Fig. 3) falls on the Zebra target and gets reflected towards the scanner (3 or 4). When the intensity of the reflected light varies owing to the movement of Zebra target, the resistance of P_c changes correspondingly causing an imbalance of bridge in proportion to change in light intensity. These changes superimposed on a trace having a fixed irate of movement are used for calculating the time of fall of the hammer.

With proper placement of top and bottom scanners (3&4) respectively (Fig 3), it is possible to monitor and record the movement of hammer as it travels up and down during each stroke. A typical data obtained during the test is shown in Fig. 5. When the hammer is being lifted up, the Zebra target passes the bottom scanner (4) which starts transmitting the changes in light intensity. The changes are recorded first on trace B (as shown at the lower end of the trace B and starting from point e). When the Zebra target has passed the bottom scanner, the trace B settles down to a smooth line. As the hammer continues its upward travel, it is picked up by the top scanner (3) at point 'a', trace T (Fig. 5). The upward journey of hammer is stopped at point 'b' after which it starts its free fall,

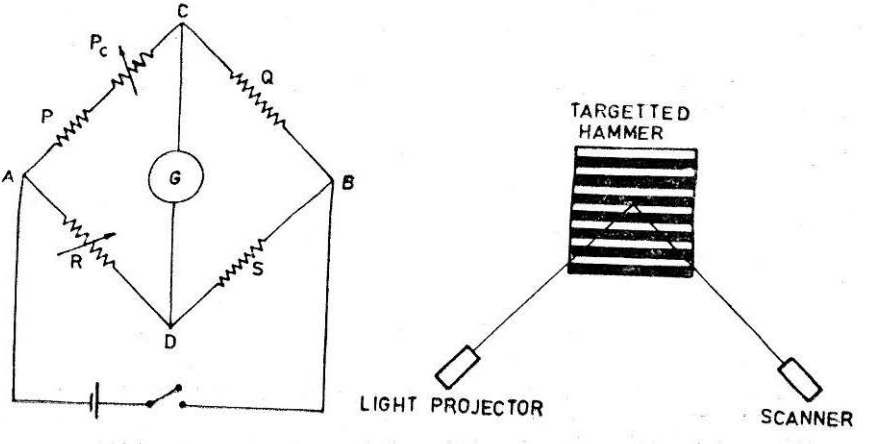

FIGURE 4 Circuit Diagram

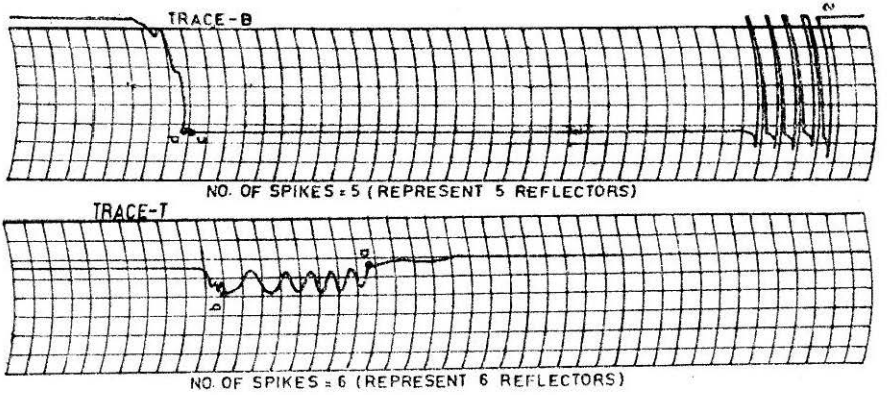

FIGURE 5 Showing the Trace of the Movement of Hammer During its Operation. The Point 'b' on trace T and Point 'd' on Trace B respectively Signify the Moments at whieh the Hammer Started its Free Fall and at which it Impacted on the Anvil.

Towards the end of free fall, the hammer is again picked up by the bottom scanner (4) (Fig. 3 at point'c' on trace B (Fig. 5). It can be observed that the hammer has 'impacted' on the anvil at point 'd' (as there is no change on trace beyond 'd').

The time of free fall of the hammer is calculated by measuring the distance between points 'b' (at which it started its free fall) and point 'd' (at which it impacted on the anvil) and dividing this distance by the rate of movement of the chart on the recording table.

Test Procedure

The test procedure consisted of placing the targeted hammer assembly on the anvil, ensuring the verticality of hammer guide rod and placing the light beam projectors and scanners close to the targeted hammer and at an angle to each other (Fig. 6*j*. The scanner frame was adjusted to vertical position and the two scanners were suitably fixed 76.2 cm apart and levelled. Before recording any observation, the amplifier record was calibrated and base lines of traces B and T (Fig. 5) were established. The hammer was hoisted during the test operations with a manila rope, 2.2 cm dia. Two turns of the manila rope were used around the winch drum of the cathead system. The hammering was carried out electrically at a speed of about 15 blows per minute.

Measurement of Fall Height

With the hammer resting on anvil, the bottom scanner was so fixed that it could see some reflector, say No. 5 in Fig. 7 (*a*) on the Zebra target. The top scanner was then fixed at a distance of 76.2 cm above the bottom scanner. The first reflector sensed by the bottom scanner is taken as reference point 'e' (Fig. 5) for evaluating the fall height. This first reflector sensed by bottom scanner should be the last reflector sensed by the top scanner (when the hammer has reached max. height and is about to drop which is evident from the increased spacing between the last two spikes and sudden change of signal at point 'b' on trace T). In case the reflector sensed last by the top scanner is not the reference reflector, then the distance between the reference reflector and last reflector sensed is the

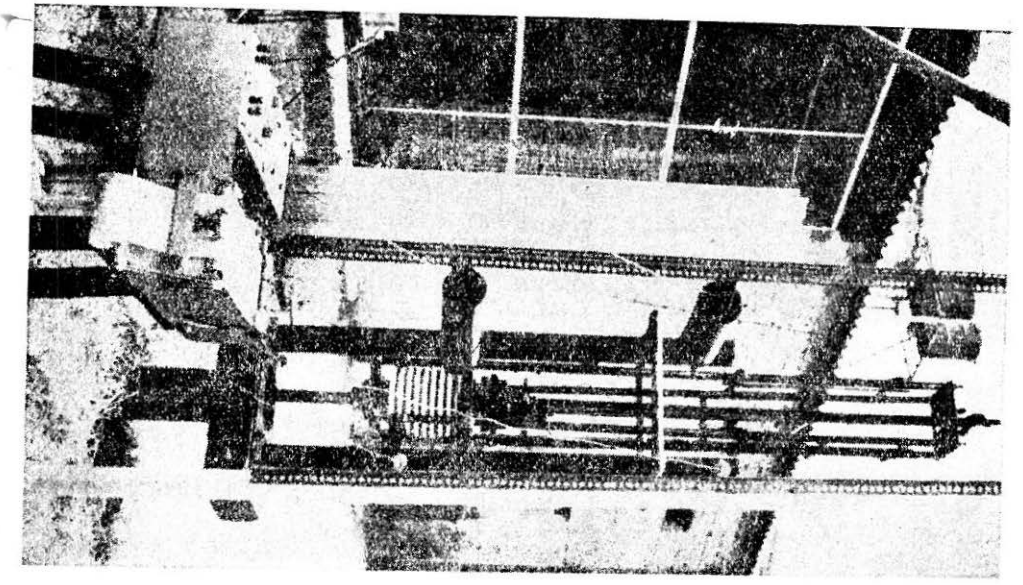

FIGURE 6 Photograph Showing the Closeup of the Test Instrumentation.

deviation from 76.2 cm fall height. For example, in Fig. 7 the first reflector sensed by the bottom scanner is 5th from bottom of Zebra target, as shown at (*a*) and is also the same reflector sensed last by top scanner, as at (*b*). Hence the fall height is exactly 76.2 cm. But in a case as shown at (*c*), if the first reflector sensed by the bottom scanner is again 5th from the bottom at (*a*) and the last reflector sensed by the top scanner (when the hammer is about to drop) is not the reference reflector (i.e. 5th) but is, say 6th from bottom as at (*c*), then, actual fall height would be 74.95 cm as the width of each reflector is 1.25 cm.

For measurement of actual fall height of the hammer during the tests, the bottom scanner was set at the centre of the 5th reflector. The top scanner was fixed exactly 76.2 cm above the bottom scanner so that for an exact 76.2 cm lift of the hammer the top scanner should see only upto the centre of the 5th reflector. A number of traced graphs were obtained during the tests. One such typical graph is shown in Fig 5. It will be observed from trace T that the top scanner has seen almost the end of 5th reflector. This indicates that the fall height of the hammer as per this trace is more than 76.2 cm but is slightly less than 76.9 cm. For demonstrating as to how the actual fall heighted, the blows up view of trace T (Fig. 5) is shown in Fig. 8 in which the position X indicates the stage when the power to the hoisting motor was switched off. The hammer along with its lifting lever assembly continued going up beyond point X because of the momentum in the system. A, B and C on the graph indicate recorded relative band widths (corresponding to the reflector bands on Zebra target) which are increasing from A to C in a definite proportion because of the retardation in the movement of the hammer against gravity. As per the proportion between the band witdhs A and B, the band widths C when the 5th reflector is seen completely by sensor should have been 26.47 mm (corresponding to 12.5 mm of band width of Zebra target). But the recorded band width C from the graph is only 26 mm which is

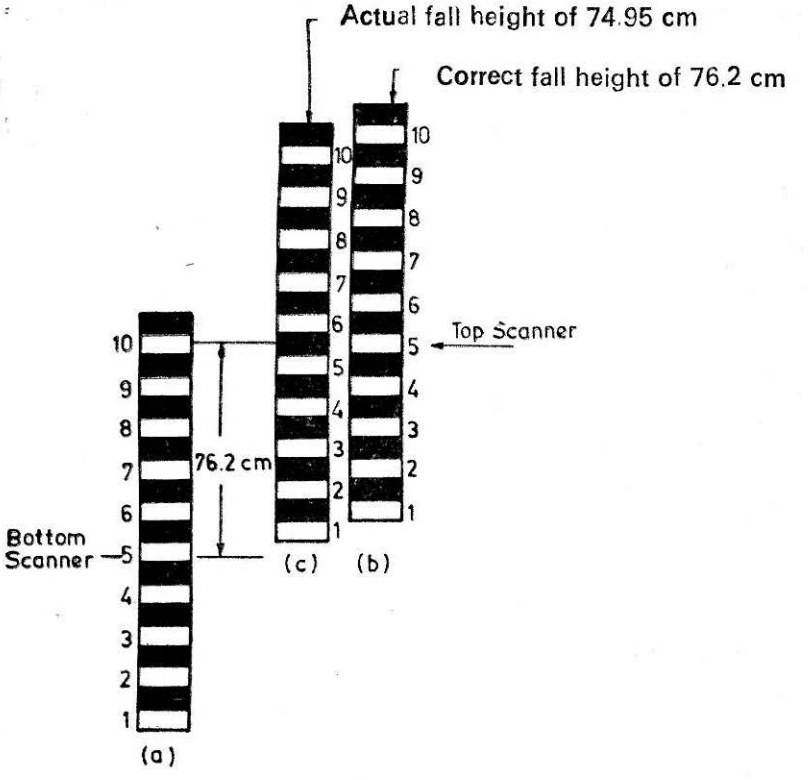

FIGURE 7 Zebra Target

indicative of the fact that the sensor has very well seen the centre of 5th reflector and also beyond that but certainly the 5th reflector has not been seen completely. The extra distance seen (or travelled up by the hammer) beyond the centre of 5th reflector (which corresponds to exactly 76.2 cm fall height) has been calculated as 6 mm which corresponds to a distance of 12.75 mm (26 mm —13.25 mm corresponding to half band width of 5th reflector) on the graph. The actual height of fall in this particular case had therefore been 76.8 cm (76.2 cm+6 mm). The average value of actual fall height calculated from different observations has been 76.7 cm.

For the calculation of actual time of fall of the hammer, the distance (in mm) between points 'b' and 'd', Fig. 5 was measured. This when divided by the rate of travel of the chart on the writing table (in mm/sec) gave the time of fall of the hammer in seconds. A number of hammer-drops were recorded and the graph of each such record was magnified to several times. For calculation purposes, a reference point X was marked on both the traces, T and B in Fig. 9. The magnification of the graph under reference was 2.1. The actual distance between points 'b' and 'd' is given by:

$$\frac{Xd - Xb}{\text{magnification}} = \frac{20.8 \text{ mm}}{2.1 \text{ mm}} = 9.904 \text{ mm}$$

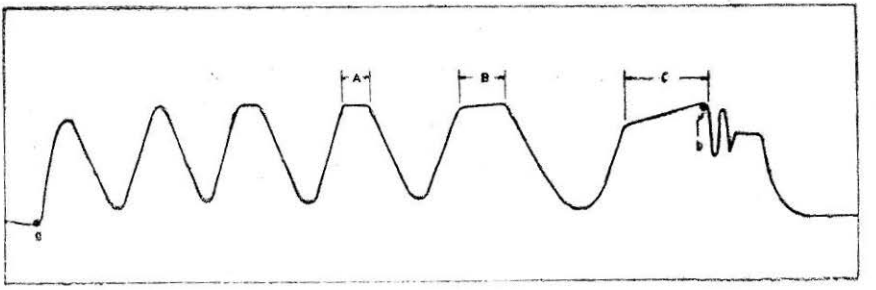

FIGURE 8 Blow-up View of Trace T of Fig. 5

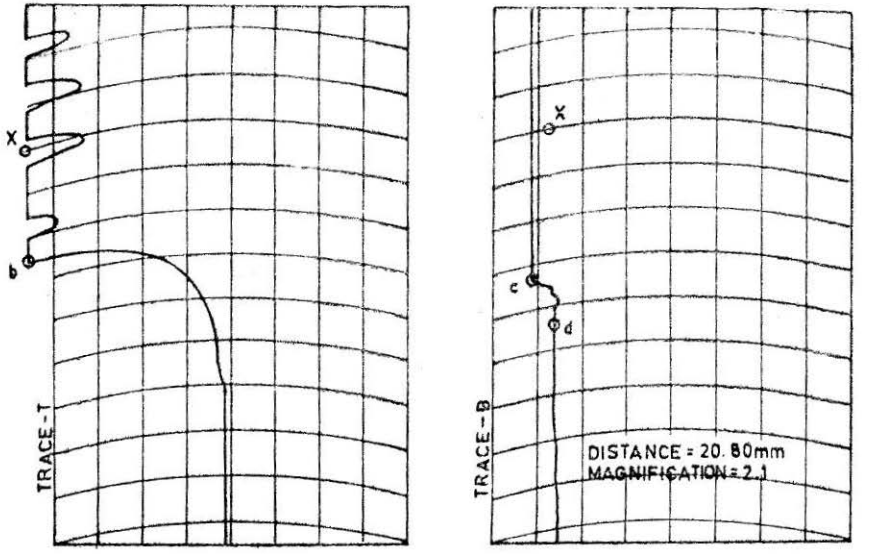

FIG. 7

FIGURE 9 A Typical Magnified Graph of the Trace of Hammer Movements. A Number of such Graphs were Obtained for Calculating the Actual Time of Fall of the Hammer.

Since the rate of chart movement over the writing table was 25 mm/sec, the time of fall was calculated to be 0.396 sec. $\left(\text{i.e. } \frac{9.904}{25}\right)$.

Results of such sixteen observations are given in Table 1. The average time of fall of hammer (t_{RC}) was calculated as 0.3995 sec. The theoretical time of fall (t_{th}) of the hammer from 76.7 cm height under true gravity fall was calculated as 0.395 sec.

Variation in Time of Fall

$$\% \text{ variation} = \frac{t_{RC} - t_{th}}{t_{th}} \times 100\ \%$$

$$= \frac{0.3995 - 0.395}{0.395} \times 100$$

$$= 1.139\ \%$$

TABLE 1

Recorded Test Data for Time of Fall of Hammer

Sl. No.	Observation No.	Magnified Distance between 'b' and 'd' (Fig.5) (mm)	Magnification	Actual distance* (mm)	Duration of fall,** (sec)
1.	2	10.05	Nil	10.05	.402
2.	3	10.00	Nil	10.00	.400
3.	4	10.1	Nil	10.1	.404
4.	5	9.9	Nil	9.9	.396
5.	6	9.9	Nil	9.9	.396
6.	7	9.9	Nil	9.9	.396
7.	8	9.9	Nil	9.9	.396
8.	A5	34.0	3.4	10.00	.400
9.	A2	21.0	2.09	10.04	.401
10.	A3	21.0	2.1	10.00	.400
11.	A6	21.0	2.09	10.04	.401
12.	A7	21.0	2.09	10.04	.401
13.	A8	34.0	3.43	9.9125	.3965
14.	A9	20.8	2.1	9.904	.396
15.	A11	21.5	2.109	10.19	.407
16.	A13	21.0	2.1	10.0	.400

Average time of fall (t_{RC}) = 6.3925/16 = 0.3995 sec.

* $\frac{\text{Magnified distance between 'b' and 'd' on graph}}{\text{Magnification}}$

** $\frac{\text{Actual distance in mm}}{\text{movement of chart (25 mm/sec)}}$

Calculation for Impact Velocity

The variation between the time for true gravity fall and the actual time recorded occured due to the friction between the moving parts of the system. The friction reduced the value of true 'g' and the effective value of acceleration due to gravity $(g)^1$ was calculated as below:

$$h = ut_{th} + 1/2\, gt_{th}^2 \qquad \ldots(1)$$

$$h = ut_{RC} + 1/2\, g^1 t^2{}_{RC} \qquad \ldots(2)$$

Comparing Equations(1) and (2),

$$g^1 = \left[\frac{t_{th}}{t_{RC}}\right]^2 \cdot g \qquad \ldots(3)$$

$$= \left[\frac{0.395}{0.3995}\right]^2 \times 981 = 959.02 \text{ cm/sec}^2$$

Theoretical impact velocity of hammer (V_{th}) $= g \times t_{th}$

$= 981 \times 0.395$

$= 387.495$ cm/sec.

Actual Impact Velocity (V) $= g^1 t_{RC} = 959.02 \times 0.3995$

$= 383.13$ cm/sec.

Comparison Between Theoretical and Actual Recorded Values of Impact K.E. (K.E$_{th}$ and K.E$_{act}$ respectively)

$$K.E_{th} = 1/2\, m\, v_{th}^2 \qquad \ldots(4)$$

$$K.E_{act} = 1/2\, m\, v^2 \qquad \ldots(5)$$

Comparing (4) and (5)

$$\frac{K.E_{th}}{K.E_{act}} = \frac{v_{th}^2}{v^2} = \frac{387.495^2}{383.13^2} = 1.022$$

$$\frac{\% \text{ variation in K.E.}}{\frac{K.E_{th} - K.E_{act}}{K.E_{th}} \times 100}$$

$$= \left(1 - \frac{(383.13)^2}{(387.495)^2}\right) \times 100$$

$= 2.241$ per cent

Energy Ratio for Velocity (ER_v)

The ratio of Kinetic energy of hammer just before impact to the potential energy of hammer is defined as the energy ratio of velocity (ER_v) (or efficiency) of the system.

$$\% ER_v = \frac{\text{Actual K.E. of impact}}{\text{P.E. (theoretical)}} = \frac{1/2 \times 63.5 \times (383.13)^2}{63.5 \times 981 \times 76.7} \times 100$$

$= 97.543$ per cent

It showed that during the performance tests the automatic free fall SPT hammer developed by CBRI registered its efficiency as 97.543 per cent which shows that the newly developed system gives reproducible fall of hammer very close to true gravity fall.

Conclusion

The automatic free fall SPT hammer system developed at CBRI promises reproducible impact force on the anvil. The fall of the hammer is very close to the true gravity fall. The system has the flexibility of operation by manual labour or by power. Major short-comings of the prevalent manual SPT method like varying height of lift of the hammer in different strokes and non-verticality of the hammer guide rod are eliminated in the newly developed system. The hammer can be used for Dynamic Cone Penetration Test (DCPT) also. The paper forms the part of normal research programme of the Central Building Research Institute and is published with the permission of the Director.

References

INDIAN STANDARDS INSTITUTION, Method for Standard Penetration Test for Soils, IS:2231-1963, Fourth Reprint, Dec. 1972.

FLETCHER, G.F.A., (1965): "Standard Penetration Test: Its Uses and Abuses", Journal of the Soil Mechanics and Foundations Division, *Proceedings of the American Society of Civil Engineers*, 91: 4: 67-75.

DINESH MOHAN, AGGARWAL, V.S. and TOLIA, D.S., (1970): Correlation of Cone Size in the Dynamic Cone Penetration Test with the Standard Penetration Test", *Geotechnique*, 20: 3: 315-319.

SANGLERAT, G. (1972): "*The Penetrometer and Soil Exploration—Development in Geotechnical Engineering*", Vol. 1 (Second Enlarged Edition), ELSEVIER SCIENTIFIC PUBLISHING CO, Amsterdam—Oxford—New York, pp. 245; 460.

SCHMERTMANN, J.H. (1978): "Use the SPT to Measure Dynamic Soil Properties,—Yes, But....." Dynamic Geotechnical Testing, ASTM STP 654, *American Society for Testing and Materials*, 341-355.

KOVACS, W.D., SALOMONE, L.A. and YOKEL, F.Y. (1981): "Energy Measurement in the Standard Penetration Test", NBS Building Science Series 135, National Bureau of Standards, Washington, DC.

KOVACS, W.D., SOLOMONE, L.A. and YOKEL, F.Y., (1983): "Comparsion of Energy Measurements in the Standard Penetration Test Using the Cathead and Rope Method" Phases I and II, final report, reparted for U.S. Nuclear Regulatory Commission, Geotechnical Engineering Group, National Bureau of Standards, Washington, DC 20324.